

Retraction

Retracted: Communication Network for Sports Activity Monitoring Systems

Complexity

Received 23 January 2024; Accepted 23 January 2024; Published 24 January 2024

Copyright © 2024 Complexity. This is an open access article distributed under the Creative Commons Attribution License, which permits unrestricted use, distribution, and reproduction in any medium, provided the original work is properly cited.

This article has been retracted by Hindawi following an investigation undertaken by the publisher [1]. This investigation has uncovered evidence of one or more of the following indicators of systematic manipulation of the publication process:

- (1) Discrepancies in scope
- (2) Discrepancies in the description of the research reported
- (3) Discrepancies between the availability of data and the research described
- (4) Inappropriate citations
- (5) Incoherent, meaningless and/or irrelevant content included in the article
- (6) Manipulated or compromised peer review

The presence of these indicators undermines our confidence in the integrity of the article's content and we cannot, therefore, vouch for its reliability. Please note that this notice is intended solely to alert readers that the content of this article is unreliable. We have not investigated whether authors were aware of or involved in the systematic manipulation of the publication process.

Wiley and Hindawi regrets that the usual quality checks did not identify these issues before publication and have since put additional measures in place to safeguard research integrity.

We wish to credit our own Research Integrity and Research Publishing teams and anonymous and named external researchers and research integrity experts for contributing to this investigation.

The corresponding author, as the representative of all authors, has been given the opportunity to register their agreement or disagreement to this retraction. We have kept a record of any response received.

References

- [1] Y. Li, L. Wan, and H. Zhang, "Communication Network for Sports Activity Monitoring Systems," *Complexity*, vol. 2021, Article ID 9971605, 10 pages, 2021.

Research Article

Communication Network for Sports Activity Monitoring Systems

Yuhua Li ¹, Lishuang Wan,² and Haimin Zhang³

¹School Regimental Committee, Henan Institute of Science and Technology, Xinxiang, Henan 453003, China

²Gangneung-Wonju National University, Gangneung-si 25457, Gangwon-do, Republic of Korea

³Institute of Physical Culture, Henan Institute of Science and Technology, Xinxiang, Henan 453003, China

Correspondence should be addressed to Yuhua Li; liyuhua@hist.edu.cn

Received 20 March 2021; Revised 6 April 2021; Accepted 10 April 2021; Published 19 April 2021

Academic Editor: Zhihan Lv

Copyright © 2021 Yuhua Li et al. This is an open access article distributed under the Creative Commons Attribution License, which permits unrestricted use, distribution, and reproduction in any medium, provided the original work is properly cited.

In this paper, through research and analysis of the communication network of the physical activity monitoring system, we combine wearable technology and identification technology and design a physical health monitoring bracelet that integrates multifaceted physical data collection and effective identity matching function. We match the identity through the chip and collect the physical fitness data generated in the process of exercise and centralized test by the sensor in real-time. Finally, the data transmission is realized through the WIFI communication function to achieve the purpose of monitoring physical exercise and improving physical quality. To ensure the continuity and stability of information transmission, the joint transmission method of direct transmission and indirect transmission is essential. Besides, considering the energy causality limitation of sensor nodes and relay nodes, a collaborative transmission model of wireless body area network based on wireless cognitive network is constructed. And, a power allocation algorithm based on maximum ratio merging and wireless cognitive network is proposed, which puts forward a new idea for the future research of wireless body area network resource allocation.

1. Introduction

With the development of the microintegrated circuit industry, chips are becoming smaller and smaller, consuming less and less energy, which leads to the production of miniature low-power smart sensors. Based on these technological advances, wireless sensor network (WSN) has facilitated the integration of healthcare and telemedicine, and these miniature low-power smart sensors can be used to monitor people's physical activity information in daily life or hospital outpatient clinics [1]. As a result, the wireless body area network (WBAN) [2] has emerged, which connects a variety of smart microsensors worn on the surface of the body or placed inside the body to continuously monitor vital physiological information in real-time. At this stage, the research of wireless body area networks still faces many challenges and difficulties, energy supply, energy consumption control, quality of service, communication distance, and security are all issues that need to be considered in the research of wireless body area networks [3]. Among

them, the energy supply problem is the primary problem of wireless body area network research, which determines the survival cycle of the network, and the way of energy supply will inevitably affect the experience of using the network [2]. The main difference between the wireless cognitive network and the previous communication network is the dynamic allocation of frequency spectrum. In order to achieve this goal, cognitive wireless networks have four processes: spectrum sensing, spectrum decision-making, spectrum sharing, and spectrum switching or mobile.

As most of the sensor nodes in the body area network have the characteristics of miniaturization. The energy density of the battery in the node is limited, and the energy that the battery can carry is very limited; once the battery energy is exhausted, the network will stop monitoring the human body, which endangers the life and property safety of users [4]. However, it is extremely inconvenient to replace the battery and charge it repeatedly regularly, especially for the sensor nodes placed inside the human body, and it is very difficult or even infeasible to replace the battery, which

seriously limits the working life of the infinite body area network [5]. In addition to hospital patient use, wireless body area network can also monitor the health of normal people, such as sports athletes, and can monitor their sports heart rate, pulse, fatigue level, and other important data in real-time, which can not only improve the efficiency of the athletes' professional training but also make the athletes' training more planned [6]. Also, wireless body area network has important applications in the daily life of the masses. In this paper, we design a physical health monitoring bracelet that combines multifaceted physical health data collection and effective identity matching in one, which can collect data generated from students' exercise process and centralized testing in real-time in many aspects to achieving the purpose of reducing accidents during sports exercise and preventing data falsification during sports testing.

Because the TCP/IP protocol is very simple and reliable, their combination determines most of the current communication methods (from wired backbone networks to hybrid networks). Now the TCP protocol has become the de facto standard for most applications. The TCP protocol was originally designed for wired networks. In wired networks, the random bit error rate is negligible. Congestion is mainly caused by packet loss. Although this mode of transmission ensures the reliable nature of network transmission, many influencing factors are redundant to consider, such as the paths that must be available for transmission from end to end and the relatively long prep time for information transmission. Wireless networks have developed rapidly in the past few years, and different intelligent classes of terminal devices have emerged one after another [7]. Mobile nodes in a mobile self-organizing network can perform various calculations independently and can communicate with each other within a known range. In addition to the above advantages, this network cannot guarantee the reliability and rate of information and data transmission compared with TCP/IP nodes, mainly due to the nature of the nodes themselves, communication range, and environment, which causes various transmission delays.

Firstly, the channel characteristics and network structure of wireless body area network are introduced, the multipoint energy and information transmission model of wireless body area network are constructed. The beamforming technique is applied in the wireless body area network, and multiple antennas are used in the transmission model AP to improve the efficiency of energy information transmission in this paper. Then, to reduce the impact of delay on energy and information transmission, delay-limited and delay-tolerant transmission models are applied to complete the communication process. Also, using the "collect-then-transmit" protocol, the throughput of the two transmission modes is investigated in depth, and the exact and asymptotic expressions of the throughput are compared to maximize the throughput and optimize the system performance. Finally, the simulation is verified by simulation.

2. Communication Network Design for Sports Activity Monitoring

2.1. Current Status of Research. The continuous development of electronic information technology has brought about more advanced wearable devices with features such as portability, high sensitivity, and low cost, which can be more easily used by people in their daily lives [8]. Wearable devices can also be called wearable computers because they can collect various data generated from people's physical activities, including motion data and physiological data, just like microcomputers [9]. Wearable devices were first invented in 1960, and the inventor was the Media Lab of MIT in the U.S. The technology was invented to facilitate people's lives, so the original wearable technology is a combination of various sensors and a master controller that allows data to be processed in a portable space and converts analog information back to digital information [10].

Pavithran et al. designed a Markov chain-based model for energy harvesting nodes in wireless body area networks based on the movement state of the human body and calculated the rate of loss of human activity information with energy consumption to provide requirements for the design of future energy harvesting nodes in wireless body area networks [11]. Yingling et al. proposed an application for cross-layer design to maximize the energy consumption of different topologies [12]. Wang et al. designed an energy-efficient data transmission strategy for wireless body area networks based on energy harvesting techniques, by which sensor nodes can select the optimal transmission power for data transmission [13]. On the basis of the above research, based on the characteristics of the small wireless body area network, combined with the limited energy during wireless body area network transmission and the low efficiency of energy information transmission [14], we consider introducing the delayed transmission mode into the wireless body area network. After derivation, analysis, simulation, and other processes, it is verified whether it can solve the problems of wireless body area network and whether it is suitable for wireless body area network [15].

Cui et al. propose a convex optimization-based combination of minimum parametric sparse arrays in wireless body area networks (WBANs) [16]. Anwar et al. discuss the combination of wireless energy and information transmission in WBANs and develop three application models to highlight key design challenges, solutions, and opportunities [17]. Bacco et al. analyze the reliability of WBANs and quantify the reliability of WBANs based on the network life cycle [18]. The reliability of WBAN is quantified based on the network life cycle and a general formula for reliability expressed in terms of the number of sensors and Group Characteristic Parameters (GCP) and upper and lower bounds for reliability are derived. Based on the monotonicity of reliability, an algorithm using the average GCP is proposed to calculate the minimum and maximum number of

sensors for a given network lifetime and the optimal number of sensors for given reliability.

2.2. Communication Network Design. Cognitive radio networks contain two types of users, primary and secondary users. Users with spectrum access licenses are primary users, which have priority to use the communication channel and do not have cognitive provisioning. Secondary users are users who are not licensed for spectrum access, cognitive users, and have cognitive provisioning. They can access the spectrum and use the communication channel only if there is no primary user, without causing any interference to the primary user, who leaves the channel when the primary user reappears. Cognitive radio users select the vacant part of the spectrum that can satisfy their transmission quality requirements.

After sensing the available spectrum bands, the subuser selects the best available spectrum band for transmission to meet its quality of service requirements, which is called spectrum decision. This process consists of three steps: in the first step, the spectrum is classified according to the detection data of the subuser, the interference level of the primary user's terminal receiver, and the path distance loss at the primary and secondary user's end; in the second step, the information is collected in a processing center, which prepares a list of available channels according to the activity requirements of the primary and secondary users; in the third step, the best channel is broadcast to the cognitive user, who adjusts its transceiver parameters to achieve communication in the available frequency bands [19].

The first type of spectrum sharing is based on spectrum type sharing and is divided into two subcategories: the first is unlicensed spectrum sharing, where all users have the same priority and secondary users can only access spectrum that is not licensed, or if the spectrum is free, the user can access the spectrum. The second type of spectrum sharing is authorized spectrum sharing, where channel access in the network is based on priority, and the primary user has a higher priority for accessing the channel, while secondary users can only access the channel without the primary user. The second type of spectrum sharing is based on network architecture sharing, which is divided into two subcategories: the first is centralized sharing, where the network processor controls spectrum access and allocation, and each user in the network forwards its requirements and information to the network processor, which thus makes spectrum allocations. The second type is distributed sharing, where distributed spectrum sharing is used where infrastructure is not available, and each node is responsible for spectrum access and allocation. The third type of spectrum sharing is access of scheme-based sharing, which is divided into two subcategories: the first is coexisting spectrum access sharing, which allows secondary users to transmit simultaneously with primary users without causing any interference to the primary users in spectrum sharing. Usually, secondary users use spread-spectrum techniques to fully utilize the spectrum and need to keep their power below an interference threshold to minimize interference to the primary user,

which is obtained by the primary receiver measuring its own received power. The second type is opportunistic spectrum access sharing, in which the secondary user opportunistically accesses the empty spectrum when the primary user is not in the spectrum. Since the secondary user uses the spectrum only in the absence of the primary user, it minimizes the impact of interference and spectrum utilization on the primary user [20–24].

A cognitive radio network architecture is given in Figure 1, which is divided into two parts: the authorized network and the cognitive network, including the primary user base station and the cognitive user base station, in addition to the primary and secondary users. The primary user in the network generally can operate certain spectrum bands, and only the primary base station can access and manage the operation, while the cognitive user has routing, transmission, MAC protocol functions, and the ability to communicate with other cognitive users. The primary base station generally cannot achieve the effect of sharing spectrum with cognitive radio users, and the cognitive user base station provides cognitive radio access services to various subusers without spectrum licenses.

From the above overview of cognitive radio, it can be seen that cognitive radio technology applied to network networking is an effective network architecture to improve spectrum utilization and alleviate spectrum shortage, which can reduce data response delay and transmission cost and improve data rate and network suitability in the network.

The openness and broadcast characteristics of wireless channels make the secure transmission of information face serious challenges. Traditional secure communication mainly encrypts data through the upper layer of the network protocol stack, and this method has inherent difficulties and weaknesses in the distribution of keys. As a supplement to the traditional encryption technology, physical layer security technology has been widely studied and printed in recent years. Physical layer security technology uses the physical layer characteristics of the channel to ensure the secure transmission of confidential information from the basic principles of information theory. Compared with traditional cryptography, physical layer security technology has the advantage of not relying on the complexity of computing, so that even if the eavesdropper is equipped with powerful computing devices, it can still ensure safe and reliable communication.

The communication channel models for wireless body area networks are body-surface-in-body, body-surface-in-body, body-surface-in-body, body-surface-body, and body-body channel models, as shown in Table 1. For the body-surface-in-body communication channel model, the other application areas have lower BER requirements and higher transmission delay and transmission rate requirements. Because in these application areas, wireless body area networks transmit more audio and video, high transmission rate and transmission delay are required to ensure user experience. However, the BER has less impact on the user experience, so the BER requirement is lower. In addition to the performance requirements of the wireless body area network introduced above, the length of service life is also an important requirement, especially in

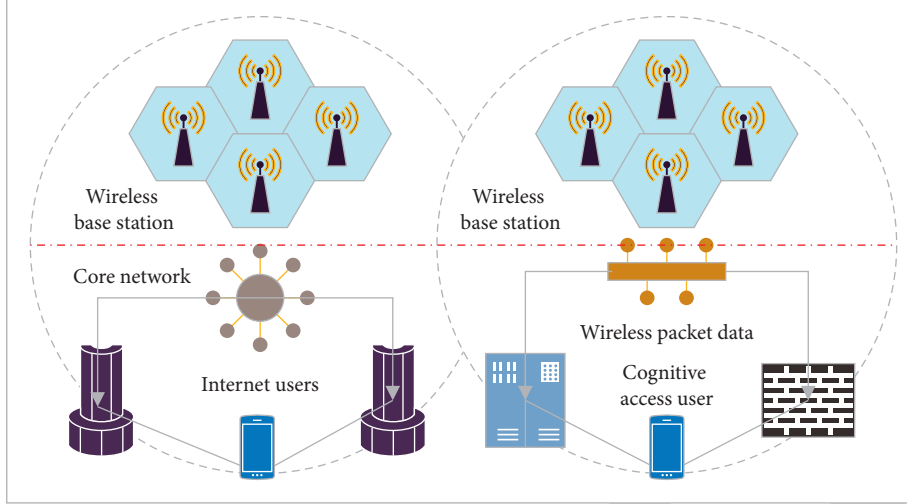


FIGURE 1: Wireless communication network architecture.

TABLE 1: Transmission path of wireless body area network.

Channel model	Frequency band
In vivo-in vivo	402–405 MHz
Body-surface	402–405 MHz
In vivo-in vitro	402–405 MHz
Body surface-body surface (LOS)	400, 600, 900 MHz, 2.4 GHz
Body surface-body surface (NLOS)	400, 600, 900 MHz, 2.4 GHz
Body surface-in vitro (LOS)	400, 600, 900 MHz, 2.4 GHz
Body surface-in vitro (NLOS)	400, 600, 900 MHz, 2.4 GHz

medical applications. A longer lifetime not only improves the user experience, but also reduces the cost of replacement and maintenance and reduces the number of WBAN maintenance by medical staff. Besides, the anti-interference and coexistence between different wireless body area networks are also gradually in the application of importance.

According to the theoretical and tested propagation models, the average received power decays logarithmically with increasing distance between the transmitting and receiving devices, and for any transmission distanced, the large-scale fading can be expressed as

$$PL(d) = PL(d_0) - 10\delta \ln\left(\frac{d}{d_0}\right) + \psi(d_0), \quad (1)$$

where $PL(d_0)$ (dB) is the path loss at the reference location d_0 , δ is the path loss index, and ψ is a Gaussian distributed random variable with mean 0 and variance δ denotes the shadow fading between the transceiver devices. This leads to the following channel coefficients between the n th RF energy tower and the k th sensor node in a multi-RF energy tower wireless body area network.

$$h_{n,k} = \sqrt{10^{(10\delta \ln(d/d_0) - \psi_{n,k}(d_0)/5)} d_{n,k}^\delta \xi_{n,k}}, \quad 1 \leq n \leq N, \quad 1 \leq k \leq K. \quad (2)$$

After the sensor nodes are replenished with energy during the WPT phase, they transmit their information data orthogonally and independently to the handheld device

within the time slots allocated by each free AP. It is assumed that the sensor nodes can use only a fixed percentage of energy for information transmission.

$$P_K = \frac{\theta_K^2 E_K^2}{t_K}. \quad (3)$$

If the data signal sent by the k -th sensor node to the handheld device is x_k , the data signal received by the handheld device from the k -th sensor node can be expressed as

$$y_{k,h} = h_{k,h} x_k - z_{k,h},$$

$$R_K = t_K w \ln\left(1 - \frac{|h_{k,h}|^2 P_K}{\delta^2}\right). \quad (4)$$

Assuming that the maximum ratio merging technique is implemented at the AP to maximize the received SNR, the final SNR at the AP can be written as

$$\gamma_A = \sum_{i=1}^K \left(\frac{\tau}{1 + \tau} \gamma_i |h_{k,h}|^2 |g_{k,h}|^2 \right). \quad (5)$$

Figure 2 shows a SWIPT network with multiple antennas Hybrid Access Point (HAP) that sends energy and information together to multiple receivers (Rx), some of which are capable of receiving both energy and information (Rx 1–4) and some of which receive only information (Rx 6) or energy (Rx 7). Because the power sensitivity of the EH receiver is -10 dB and the power sensitivity of the ID receiver is -60 dB, the EH receiver is closer to the transmitter than the D receiver in the case of effective energy reception. Because the waveform generated by the transmitter HAP directly determines the performance of energy and information transmission, so to maximize the efficiency of information (energy) transmission in extreme cases, HAP can ignore the energy (information) receiver and optimize the waveform. However, this imbalanced design may result in poor energy and information transfer performance due to

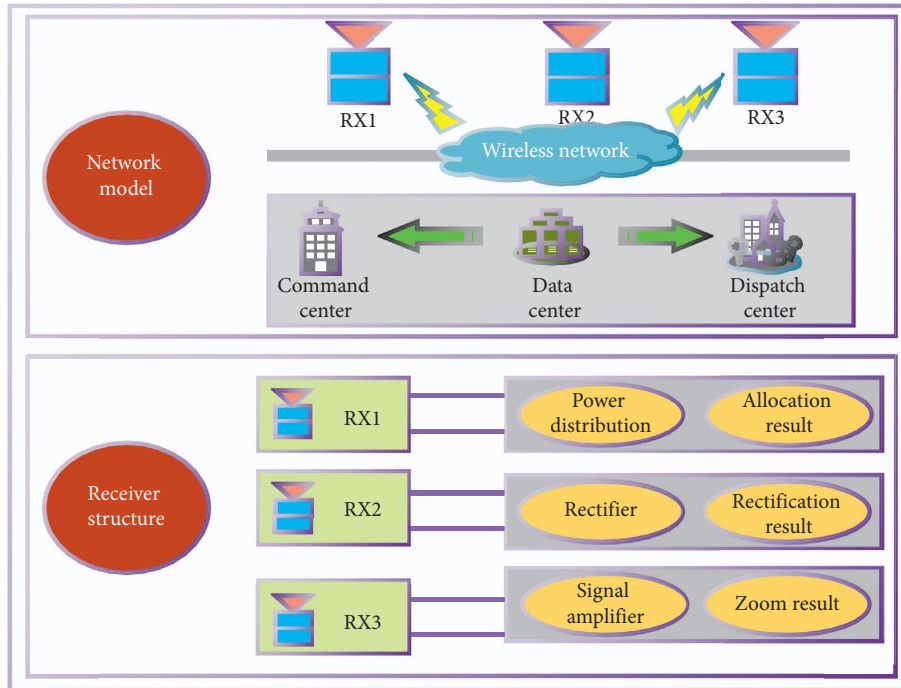


FIGURE 2: SWIPT network model and receiver structure.

the fundamental differences in the optimal waveforms for energy and information transfer. To achieve the optimal rate-energy trade-off, the waveform design for energy and information transmission needs to follow the rate-energy trade-off, while the receiver structure and corresponding signal processing can influence the characterization of the rate-energy trade-off. An ideal SWIPT receiver capable of decoding information and deriving energy from the same signal cannot be achieved by actual circuitry.

As in Figure 2, the TS receiver Rx 1, EH, and ID receivers form a TS receiver by copositioning, where the ID receiver is a conventional message decoding receiver. The HAP transmits energy and information to Rx 1 by dividing the transmission block into two orthogonal time slots for transmitting energy and information and can optimize the transmitted waveform in each time slot. Therefore, the Rx 1 receiver can periodically switch between the two-time slots for collecting energy and decoding information and then achieve different rate-energy (R-E) trade-offs by changing the length of the energy transfer slot.

Besides setting the optimal duration of WET in the first stage, another important issue in the collect-then-transmit protocol is to design an effective multiple-access scheme to coordinate the user UL information transmission in the second stage. In previous wireless communication systems, the information transmission rate of sensors far away from the HAP is lower compared to sensors near the HAP. This fairness issue is a difficult and important point in wireless communication networks. Because of significant signal attenuation, sensors far from the HAP (U) harvest lower wireless energy in the DL but consume more energy to transmit information in the UL than sensors in the vicinity of the HAP (U).

2.3. Design of the Physical Activity Monitoring System. The software design includes the program design of the main control module and the program design of each functional module, as shown in Figure 3, which shows the software workflow of the system. Based on the NRF51822 on-chip interface, the main control module is designed to collect and process physiological data, establish WIFI communication with the application side, send and receive data packets, and update the display of the bracelet in real-time.

In this model, relay nodes use time allocation protocols or power allocation protocols to decode information and collect energy and then use the collected energy to assist in the forwarding of information. Collaborative transmission not only extends the network transmission distance but also increases the system throughput and capacity. It is an important transmission technology of great interest to both academia and industry. Relay nodes applied in wireless body area networks are usually responsible for the bit-by-bit transmission of information on the physical layer between the destination and source nodes in case of poor channel state or uneven resource allocation of multiple sensor nodes. In this paper, the decode-and-forward collaborative transmission will be used as the relay transmission method. Wireless body area networks are short-range communication networks, so the introduction of relay transmission will greatly increase the channel state originating from between relay nodes, and it can also avoid the interference caused by signals from multiple sensor nodes to the source node to a certain extent.

To solve the partial collision phenomenon of PA algorithm, SA algorithm was developed, which divides the time into many discrete time slots based on the PA algorithm and divides the time slots into three types of time slots: successful time slots, collision time slots, and idle time slots according

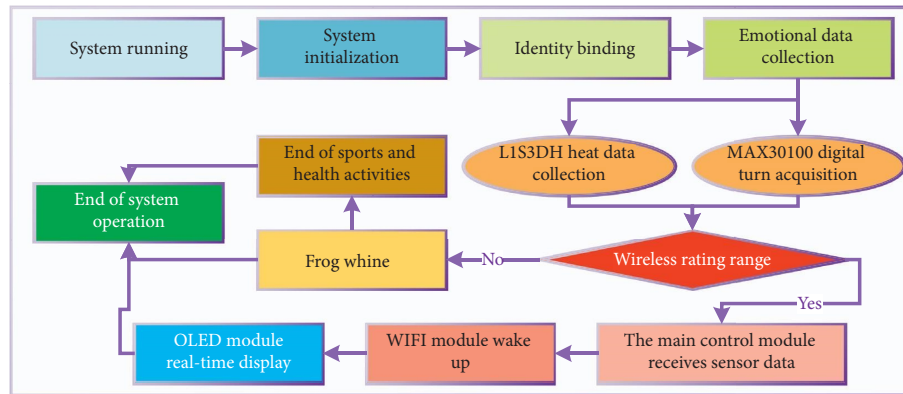


FIGURE 3: System workflow diagram.

to the number of signals returned by the tag. The length of the time slot must be greater than the time required for data transmission. The tag is successfully recognized in the success time slot, and the tag sends data in the idle time slot; in the collision time slot, the tag collision occurs due to multiple tags sending data at the same time, and the system randomly delays several time slots before the collision re-sends data until all tags are successfully recognized by the reader, and the algorithm ends.

After recognizing the tag information, the reader sends an answer signal to the corresponding tag, and the corresponding tag enters the dormant state, and the algorithm ends when all tags are recognized successfully. Because of the PA algorithm, the tags send data at random times, and the signal sending times of multiple tags partially overlap, which leads to the interference of the data sent between tags. There is a partial collision. Therefore, it has a very low throughput rate of only 18.4%.

In a wireless body area network, all sensor nodes are placed inside or on the surface of the human body, and the nodes are not far from each other, so the distance between all sensor nodes and RF energy towers or handheld devices is almost the same, and the inequity problem seems to be eliminated on the surface. However, it should be noted that the unfair problem arises fundamentally because of the difference in channel conditions between nodes, and in wireless body area networks, human organs, extremities, and clothing all produce more severe shadow fading, making the channel conditions of sensor nodes vary greatly. Therefore, unfairness still exists in wireless body area networks, and the unfairness of throughput distribution among sensor nodes can affect user experience and even threaten the life safety of users, so it is an urgent problem to be solved.

The data values are displayed on the ICD display, while an alarm is triggered if the data is out of the normal range. The stored values are sent to the server with help. All the values are stored on the server in chronological order, and the monitor can log in to view the data of the monitored person through the login credentials, and then it can grasp the athlete's body temperature and heart rate during exercise in real-time, monitor his physical condition during exercise, and effectively avoid

sports accidents. This data can also be used to develop individual training plans to achieve the best sports training results.

3. Results and Analysis

3.1. Analysis of Communication Network Performance Test Results. In this section, the proposed throughput is simulated and verified by MATLAB in the delay-tolerant transmission mode. Besides, the optimal system throughput is derived and the system performance is optimized by comparing and analyzing with the delay-tolerant and delay-limited transmission modes under the same simulation conditions, provided that the delay-tolerant and delay-limited transmission modes are known to be different. In all the following simulations, multiple equidistant sensors, we set the distance between AP and sensor U; multiple unequal distance sensors, we simulate based on the data provided; AP uses mid-waist node, other ten parts nodes as sensor nodes. The channel model $Q = 10^3$, path loss index $\alpha = 2$, and energy harvesting efficiency $n = 0.6$.

Figure 4 plots the relationship between the average AP throughput and AP transmit power for different numbers of antennas under a single sensor. For the delay-tolerant mode, the asymptotic throughput rapidly approaches the exact throughput as the AP transmit power increases, although there is a gap between the two when the transmit power is low. The figure also shows that the system throughput in the delay-tolerant mode improves as the transmit power or the number of antennas increases.

Figure 5 shows the effect of the number of antennas on the AP on the system throughput at different energy harvesting times under a single sensor. As the number of antennas becomes larger in the delay-tolerant mode, the system throughput increases accordingly. However, the slope of the throughput curve gradually decreases, which is consistent with our theoretical analysis because the average throughput is proportional to the psi function of the number of antennas. Also, the energy harvesting time shown in Figure 5 does not affect the system throughput as much as the number of antennas for the delay-tolerant mode. For

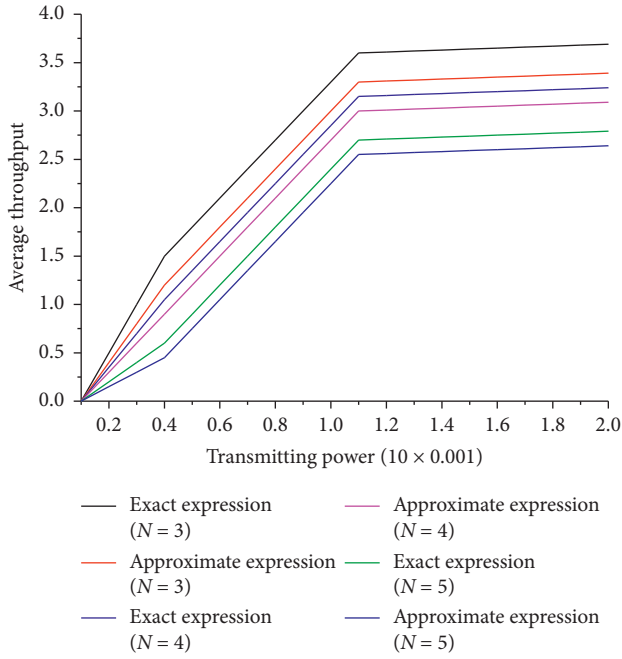


FIGURE 4: Schematic of single sensor throughput with P .

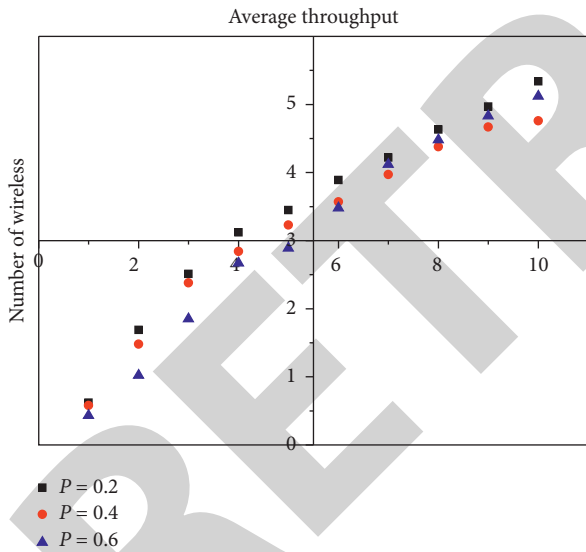


FIGURE 5: Schematic of the average throughput of a single sensor with N .

example, when the value increases from 0.2 to 0.4, the throughput in delay-tolerant mode is improved. However, when increasing from 0.4 to 0.6, the system throughput decreases significantly for $N \geq 2$.

The total throughput obtained by all sensor nodes at 5 different locations is shown in Figure 6, and the throughput obtained by each sensor node at 5 different locations is shown in Figure 6. As seen in Figure 6, the system can obtain a great total throughput with a minimum throughput of 21 Mbit/s. The difference between the total throughput obtained by the sensor nodes at locations 2, 3, 4, and

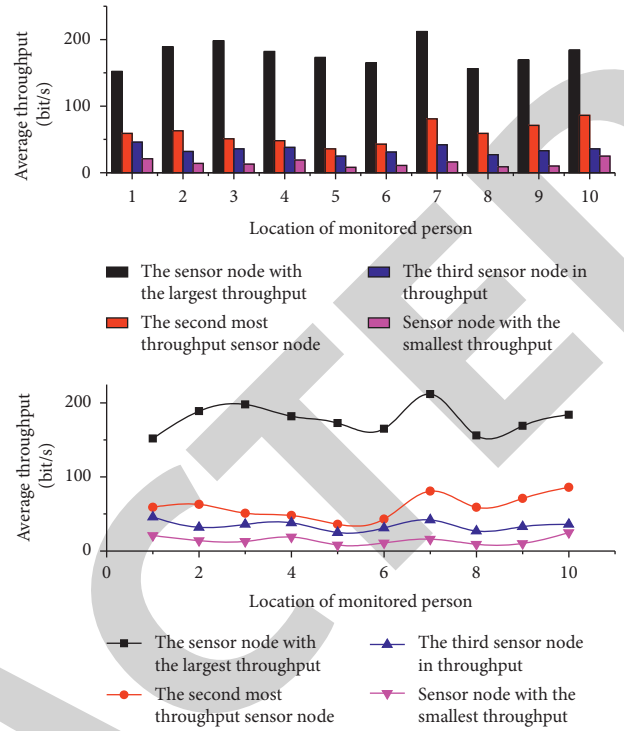


FIGURE 6: Total system throughput under the throughput maximization mechanism and throughput of each sensor node under the throughput maximization mechanism.

locations 1 and 5 is larger, close to 2 Mbit/s. This is because the sensor nodes at locations 2, 3, and 4 are closer to all RF energy towers and can collect a more enough energy, so they can obtain a larger throughput. While at locations 1 and 5, the sensor nodes are far from some of the RF energy towers and collect relatively less energy, so the throughput obtained is also smaller. In Figure 6, the four rectangular bars at each of the five locations indicate the throughput of the four sensor nodes, and for the convenience of analysis and comparison, the sensor nodes are arranged in descending order by their throughput in this paper. As can be seen from the figure, the difference in throughput obtained by each sensor node at each of the 5 positions is large, with the maximum throughput being 17 times greater than the minimum throughput.

The average fairness index does not float very much in the 5 positions, but the values are small, mainly jittering above and below 0.374. Due to the randomness of patient posture and clothing, which leads to the greater randomness of invisible fading, and the total throughput maximization mechanism ignores the fairness of the system and does not control the fairness of resource allocation, the average fairness index does not change regularly in 5 positions. From the above three figures, it can be seen that although the total throughput maximization mechanism can obtain a great total throughput and effectively improve the efficiency of the system, the fairness of the system is extremely low, and the throughput gap between sensor nodes is extremely large. This is because the total throughput maximization mechanism allocates more network resources to sensor nodes with

better channel conditions to maximize the system efficiency, ignoring the throughput demand of sensor nodes with poor channel conditions, resulting in a serious inequity in network resource allocation.

The total throughput maximization mechanism enables the system to obtain a great total throughput, but the fairness of the system is extremely low. The forced equal throughput mechanism, although effective in improving the fairness of the system, severely loses too much system efficiency. Both resource allocation mechanisms sacrifice some of the sensor nodes' efficiency; the former allocates fewer resources to sensor nodes with poor channel conditions to obtain a very small throughput, while the latter reduces the resources occupied by sensor nodes with good channel conditions to reduce the throughput they can obtain.

3.2. Analysis of Monitoring System Performance Test Results. The heart rate measurement method used in the MAX30100 sensor is a photoelectric transmission, which uses the difference in light absorption between oxygen-carrying hemoglobin and non-oxygen-carrying hemoglobin in the blood vessels to achieve the measurement. The light source generally consists of two types of LEDs: a visible red light with a wavelength of 660 nm and near-infrared light with a wavelength of 940 nm. The LED light emitted inside the sensor will pass through the body's light-transmitting layer and the light transmission rate will change with the arterial pulsation filling volume changes; at this time the MAX30100 built-in photoelectric converter will receive the light reflected by the body's tissue and will be converted into electrical signals and then amplified and output. Figure 7 is the hemoglobin absorption spectrum.

This chapter uses the IC communication interface to directly read the MAX30100 internal memory; the specific workflow includes the following: first select COM3 port open, select the baud rate of 38400, and select the parity bit for no parity. The final collected data is output to the computer through the serial port, where raw RedValue and raw IRValue are the raw data collected by the red LED and infrared LED, respectively.

Figure 8 shows the energy efficiency versus the number of channels N over the channel count interval 0 to 125, which shows that as the number of channels N increases, the energy efficiency increases rapidly. The reason for this phenomenon is that as the number of channels available in the network increases, it allows more flexibility in the allocation of channels to subusers in the network, thus achieving higher energy efficiency. It is also shown that the algorithm proposed in this chapter achieves the highest energy efficiency compared to the three reference algorithms, and the value of energy efficiency improvement becomes larger as the number of assignable channels in the network becomes larger. This indicates that the algorithm presented in this chapter is particularly effective when the number of assignable channels in the network is large.

This paper introduces two network architectures for the application of wireless energy transfer technology in thrust less communication networks and analyses the differences between the two architectures. To minimize the unfairness of

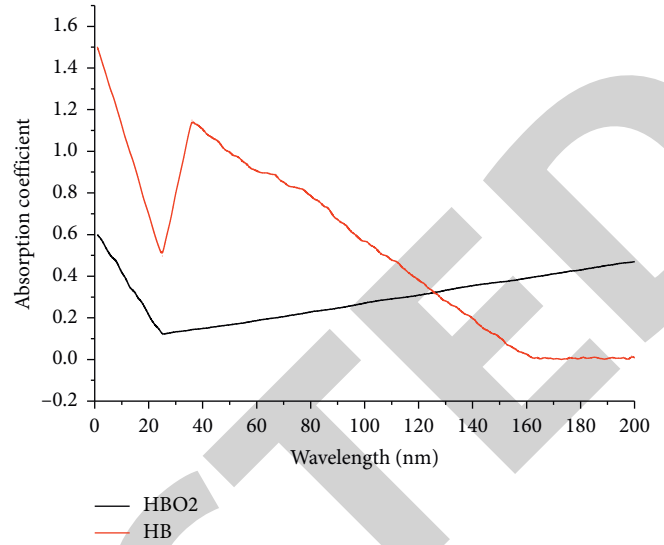


FIGURE 7: Hemoglobin absorption spectrum.

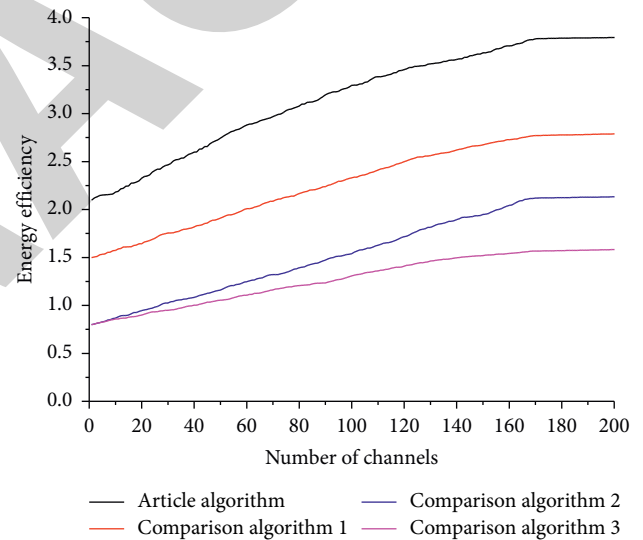


FIGURE 8: Energy efficiency versus the number of channels N .

the network, this paper adopts the hetero structure as the network structure of the studied system model. Also, this paper improves the system model in the existing research results and proposes a system model of wireless charging body area network with multiple RF energy towers and establishes the model of energy and information transmission based on this system model. This system model can provide more sufficient energy for sensor nodes to ensure their stable and continuous work and has certain practicality.

4. Conclusion

This paper focuses on the problem of network resource allocation in multipoint classified wireless body area networks based on RF energy transmission. Considering the

shadow fading generated by the human body and clothing, a multisensor node wireless body area network that communicates only through direct transmission is prone to interruption of communication. For wireless body area networks with high requirements for reliability and continuity of information transmission, a system model of multisensor node wireless body area network with a combination of direct transmission and relay transmission is more practical. In this paper, we first propose a collaborative transmission model for multisensor node wireless body area networks. However, the data collected by any sensor node is very important reference information for both the wearer and the medical personnel. From a medical point of view, a new type of classified wireless body area network model is proposed by grouping multiple sensors according to the detected signals and according to the location of the human body where the same group of sensors can transmit common information. A pricing-based method for allocating energy resources in cooperative cognitive wireless energy supply communication networks is proposed. A multicarrier collaborative cognitive wireless energy supply communication network is considered, which contains a cognitive base station and multiple subusers that share the spectrum of a wireless energy supply primary user. By evaluating the outage probability and traversal capacity at a given energy collection time, we investigate the average throughput expressions for each of the two delayed transmission modes. Also, the two delayed transmission modes are compared by simulation, and the throughput of the delay-tolerant transmission mode outperforms the delay-constrained transmission mode in some cases.

Data Availability

The data used to support the findings of this study are available from the corresponding author upon request.

Conflicts of Interest

The authors declare that they have no conflicts of interest regarding the publication of this paper.

References

- [1] M. T. Arefin, M. H. Ali, and A. K. M. F. Haque, "Wireless body area network: an overview and various applications," *Journal of Computer and Communications*, vol. 5, no. 7, pp. 53–64, 2017.
- [2] B. Sharma and D. Koundal, "Cattle health monitoring system using wireless sensor network: a survey from innovation perspective," *IET Wireless Sensor Systems*, vol. 8, no. 4, pp. 143–151, 2018.
- [3] L. P. Malasinghe, N. Ramzan, and K. Dahal, "Remote patient monitoring: a comprehensive study," *Journal of Ambient Intelligence and Humanized Computing*, vol. 10, no. 1, pp. 57–76, 2019.
- [4] R. Punj and R. Kumar, "Technological aspects of WBANs for health monitoring: a comprehensive review," *Wireless Networks*, vol. 25, no. 3, pp. 1125–1157, 2019.
- [5] S. Hara, H. Yomo, R. Miyamoto et al., "Challenges in real-time vital signs monitoring for persons during exercises," *International Journal of Wireless Information Networks*, vol. 24, no. 2, pp. 91–108, 2017.
- [6] K. E. Friedl, "Military applications of soldier physiological monitoring," *Journal of Science and Medicine in Sport*, vol. 21, no. 11, pp. 1147–1153, 2018.
- [7] M. Ha, S. Lim, and H. Ko, "Wearable and flexible sensors for user-interactive health-monitoring devices," *Journal of Materials Chemistry B*, vol. 6, no. 24, pp. 4043–4064, 2018.
- [8] U. Satija, B. Ramkumar, and M. Sabarimalai Manikandan, "Real-time signal quality-aware ECG telemetry system for IoT-based health care monitoring," *IEEE Internet of Things Journal*, vol. 4, no. 3, pp. 815–823, 2017.
- [9] M. Devarajan, V. Subramaniaswamy, V. Vijayakumar, and L. Ravi, "Fog-assisted personalized healthcare-support system for remote patients with diabetes," *Journal of Ambient Intelligence and Humanized Computing*, vol. 10, no. 10, pp. 3747–3760, 2019.
- [10] A. Kos and A. Umek, "Wearable sensor devices for prevention and rehabilitation in healthcare: swimming exercise with real-time therapist feedback," *IEEE Internet of Things Journal*, vol. 6, no. 2, pp. 1331–1341, 2019.
- [11] D. Pavithran, K. Shaalan, J. N. Al-Karaki, and A. Gawanmeh, "Towards building a blockchain framework for IoT," *Cluster Computing*, vol. 23, no. 3, pp. 2089–2103, 2020.
- [12] L. R. Yingling, V. Mitchell, C. R. Ayers et al., "Adherence with physical activity monitoring wearable devices in a community-based population: observations from the Washington, D.C., Cardiovascular Health and Needs Assessment," *Translational Behavioral Medicine*, vol. 7, no. 4, pp. 719–730, 2017.
- [13] D. Wang, Y. Guo, S. Liu, Y. Zhang, W. Xu, and J. Xia, "Haptic display for virtual reality: progress and challenges," *Virtual Reality & Intelligent Hardware*, vol. 1, no. 2, pp. 136–162, 2019.
- [14] Y. H. Lee, O. Y. Kweon, H. Kim, J. H. Yoo, S. G. Han, and J. H. Oh, "Recent advances in organic sensors for health self-monitoring systems," *Journal of Materials Chemistry C*, vol. 6, no. 32, pp. 8569–8612, 2018.
- [15] J. Breda, J. Jakovljevic, G. Rathmes et al., "Promoting health-enhancing physical activity in Europe: current state of surveillance, policy development and implementation," *Health Policy*, vol. 122, no. 5, pp. 519–527, 2018.
- [16] D. Cui, J. C. Drake, R. J. Wilson et al., "A novel voluntary weightlifting model in mice promotes muscle adaptation and insulin sensitivity with simultaneous enhancement of autophagy and mTOR pathway," *The FASEB Journal*, vol. 34, no. 6, pp. 7330–7344, 2020.
- [17] M. Anwar, A. H. Abdullah, K. N. Qureshi, and A. H. Majid, "Wireless body area networks for healthcare applications: an overview," *TELKOMNIKA (Telecommunication Computing Electronics and Control)*, vol. 15, no. 3, pp. 1088–1095, 2017.
- [18] M. Bacco, F. Delmastro, E. Ferro, and A. Gotta, "Environmental monitoring for smart cities," *IEEE Sensors Journal*, vol. 17, no. 23, pp. 7767–7774, 2017.
- [19] S. Niu, N. Matsuhisa, L. Beker et al., "A wireless body area sensor network based on stretchable passive tags," *Nature Electronics*, vol. 2, no. 8, pp. 361–368, 2019.
- [20] M. Bassoli, V. Bianchi, I. De Munari, and P. Ciampolini, "An IoT approach for an AAL Wi-Fi-based monitoring system," *IEEE Transactions on Instrumentation and Measurement*, vol. 66, no. 12, pp. 3200–3209, 2017.
- [21] B. Yong, W. Wei, K. C. Li et al., "Ensemble machine learning approaches for webshell detection in Internet of things environments," *Transactions on Emerging Telecommunications Technologies*, p. e4085, 2020.

- [22] X. Fan, F. Du, and W. Wei, "A geography-based void-bypassing routing protocol for wireless sensor network," *Wireless Personal Communications*, vol. 90, no. 1, pp. 259–280, 2016.
- [23] W. Wang, N. Kumar, J. Chen et al., "Realizing the potential of the internet of things for smart tourism with 5G and AI," *IEEE Network*, vol. 34, no. 6, pp. 295–301, 2020.
- [24] J. Yang, C. Wang, B. Jiang, H. Song, and Q. Meng, "Visual perception enabled industry intelligence: state of the art, challenges and prospects," *IEEE Transactions on Industrial Informatics*, vol. 17, no. 3, pp. 2204–2219, 2021.

RETRACTED